EUROPEAN ORGANIZATION FOR NUCLEAR RESEARCH

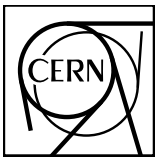

ALICE-PUBLIC-2025-006

European Strategy for Particle Physics 2026: Frontier sensor R&D for the ALICE 3 apparatus

ALICE Collaboration

Abstract

The ALICE Collaboration plans to build a new experimental setup, ALICE 3, which will be installed during Long Shutdown 4. This apparatus will maximize the potential of the HL-LHC as a heavy-ion collider by giving access to new and unexplored experimental observables, thereby enabling the investigation of open fundamental questions regarding the quark-gluon plasma and other aspects of the strong interaction. The hallmarks of the ALICE 3 physics programme are discussed in a dedicated ESPP input document. They require unprecedented pointing resolution (e.g. about 10 μm at $p_{\mathrm{T}} = 250$ MeV/c), large acceptance ($|\eta| < 4$ and $p_{\mathrm{T}} > 50$ MeV/c) and extensive identification capabilities for electrons, hadrons and muons. The setup consists of a compact silicon pixel tracker within a new superconducting magnet (2 T), silicon time-of-flight layers, a ring-imaging Cherenkov detector, a muon identification system, an electromagnetic calorimeter, a forward photon conversion tracker, and two forward counting detectors. An intense R&D programme on frontier sensors is well underway. The primary focus of the R&D on Monolithic Active Pixel Sensors for the trackers is on high spatial precision, low material budget, low power consumption, and large-area sensors. A pioneering concept is being pursued for a retractable barrel vertex detector that closes to a minimum radius of 5 mm from the interaction point. For particle identification, R&D is in progress towards ultra-fast timing with silicon sensors for time-of-flight measurement, and towards improving the radiation hardness of silicon photo-multipliers. The target specifications of the ALICE 3 silicon sensors are similar to those of detectors at future colliders. The advancements in sensor technologies targeted by the ALICE 3 R&D programme constitute a significant milestone in the ECFA strategic roadmap for detector R&D.

1 Introduction

The goal of the ALICE physics programme is to determine the properties of the quark–gluon plasma (QGP), the deconfined state of strongly-interacting matter. While significant progress is expected from the LHC programme of Run 3 and Run 4 (until 2033), a number of fundamental questions on the QGP and other aspects of the strong interaction will remain open. In order to address these questions and to fully exploit the potential of the high-luminosity LHC as a heavy-ion collider during Runs 5 and 6, as recommended by the 2020 update of the European Strategy for Particle Physics, a completely new setup ALICE 3 is proposed as part of the Phase IIb Upgrades of the LHC experiments during the fourth long shutdown (LS4, 2034–2035) [1].

The ALICE 3 apparatus (Fig. 1) consists of a silicon-pixel tracking system with unique pointing resolution over a large pseudorapidity range ($-4 < \eta < +4$), complemented by systems for particle identification, from ultra-low to intermediate momentum, including silicon time-of-flight layers (TOF), a ring-imaging Cherenkov detector (RICH), a muon identification system (MID), an electromagnetic calorimeter (ECal), a forward photon conversion tracker (FCT), and two forward counting detectors (FD). A new superconducting solenoid magnet with a field strength of 2 T provides a transverse momentum resolution similar to that of the present ALICE detector in the central region, as well as good momentum resolution at forward rapidity.

The Scoping Document for ALICE 3 [2] has recently been reviewed by the LHC Committee (LHCC). R&D for these detectors has started three years ago and is intensifying in preparation of Technical Design Reports. The two main aspects of the R&D studies are the development and selection of sensors and readout ASICs, and the design of full detector systems, including sensors, readout, and all services (mechanical supports, cooling, powering, data links, etc.). The target specifications for the trackers, TOF and RICH detectors, in terms of spatial and timing resolution, material budget, and radiation tolerance for the full Run 5 integrated luminosities of 18 fb^{-1} and 33.6 nb^{-1} in pp and Pb–Pb, respectively, demand frontier R&D beyond the presently-available silicon sensors. The specifications and the R&D lines for these subsystems are the main focus of this document and they are reported in Sections 2 and 3. For completeness,

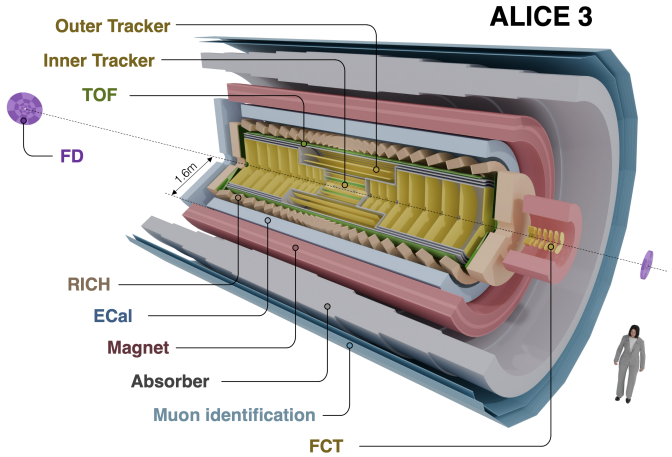

Figure 1: ALICE 3 detector layout (corresponding to version 1 of the Scoping Document [2]).

the sensor options and R&D plans for the other ALICE 3 subsystems are summarised as well (Section 4). The frontier R&D for the ALICE 3 silicon-based sensors matches some of the most ambitious goals defined in the European Committee for Future Accelerators (ECFA) roadmap for detector R&D [3]. This is due to many of the specifications being similar to, or more stringent than, those for experiments at future colliders, such as FCC-ee and EIC. Therefore, the advancements achieved in the next five years in preparation for ALICE 3 will have a clear benefit on the developments for the further future and can serve as a concrete mid-term milestone in the longer term roadmap. This item is discussed in Section 5.

2 ALICE 3 subsystems based on silicon sensors

2.1 Silicon-pixel trackers

The core ALICE 3 detector component is a large silicon tracker consisting of CMOS Monolithic Active Pixel Sensors (MAPS) arranged in 11 barrel layers, 12 forward and 12 backward disks, covering a total area of 56 m^2 and a pseudorapidity acceptance $|\eta| < 4$, thinned down to between 30 and 100 μm depending on the radial position.

The Inner Tracker (IT) includes the three innermost layers and disks (Vertex Detector), plus the following four Middle Layers (ML) up to a radius of 20 cm, and six small disks at longitudinal distances z ranging from $\pm$77 cm up to $\pm$122 cm. The Vertex Detector (VD), similarly to the ITS3 concept [4], consists of bent wafer-scale silicon pixel sensors placed inside the beam pipe. It features ultra-low material budget and, being retractable, can be closed to an innermost radius of 5 mm after beam stabilisation, thus providing a track pointing resolution of $\sim$10 μm at $p_{\mathrm{T}} = 250$ MeV/c and $\sim$4–5 μm at $p_{\mathrm{T}} = 1$ GeV/c over the full η acceptance.

The Outer Tracker (OT) consists of the four outermost layers, located at radii between 30 cm and 80 cm, and of the twelve large disks at longitudinal distances z ranging from $\pm$150 cm up to $\pm$350 cm.

The FCT covers $4 < \eta < 5$ at $442 < z < 500$ cm and consists of eleven disks similar to those of the ML, but with a smaller radius of $\sim$ 18 cm.

2.1.1 Specifications

The main specifications of the tracker sensors are given in Tab. 1.

Table 1: Tracker sensors specifications.

	VD	ML	OT	FCT
Area (m^2)	0.15	5.6	50.4	0.35
Spatial resolution (μm)	2.5	10	10	10
Hit rate (MHz/cm^2)	96	0.6	0.6	0.6
Material budget per layer ($\%X_0$)	0.1	1	1	1
Power density (mW/cm^2)	70	20	20	20
Time resolution (ns)	100	100	100	100
Radiation tolerance NIEL (1 MeV n_{eq}/cm^2)	$1.0 \cdot 10^{16}$	$2 \cdot 10^{14}$	$6 \cdot 10^{12}$	$5 \cdot 10^{13}$
Radiation tolerance TID (rad)	$3 \cdot 10^{8}$	$5 \cdot 10^{6}$	$2 \cdot 10^{5}$	$2 \cdot 10^{6}$

2.1.2 Baseline sensors and additional options

The baseline technology for the VD and the ML+OT MAPS is the 65-nm CMOS imaging process, which is also the choice for the ongoing ITS3 [4] development.

Option with curved sensors in the ML

For the ML, the possibility of using wafer-scale bent sensors is being explored. This would represent a further development of the ITS3 concept, adapted to cover a larger surface. Such a concept has the potential to significantly reduce the material budget of the relevant layers and move the first hit point, which is located outside the beam pipe, closer to the interaction point. However, this approach has a considerable impact on the detector assembly and integration process, as well as on the overall cost, compared to planar sensor ladders. Therefore, it is better suited for applications that require limited active area coverage, as is the case with the ML.

Option with timing for PID in the outermost IT layer

One option currently under consideration is the addition of time measurement capabilities to the outermost barrel layer of the ML, located at a radius of about 20 cm. This would enable the replacement of the inner TOF layer (see Section 2.2) with a single 4D tracking layer that combines both tracking and timing capabilities. Results obtained from the APTS-OA prototype during the ITS3 MLR1 run show a promising time resolution of 63 ps [5, 6]. To achieve the required radiation hardness and reduce power consumption, further optimizations are needed for the pixel capacitance and charge-collection properties. These improvements could potentially enhance the timing performance, bringing it closer to the required 20 ps resolution [7]. Importantly, such developments would not affect the program for the outer barrel and disks of the TOF system.

2.1.3 R&D plans

The R&D for the IT is challenging with regard to pixel detector technology, mechanical engineering and integration of services.

The R&D for the pixel chip will be a continuation of the work ongoing for the ALICE ITS3 and will focus on highly demanding requirements on radiation tolerance, small pixel size and data rates. ITS3 sensor prototypes demonstrated close to full efficiency after irradiation with 1×10^{15} 1 MeV $n_{\mathrm{eq}}/\mathrm{cm}^2$ or 10 Mrad at room temperature [8]. The innermost layer of the VD will receive a lifetime Non Ionizing Energy Loss (NIEL) dose of the order of 1×10^{16} 1 MeV $n_{\mathrm{eq}}/\mathrm{cm}^2$ and a Total Ionizing Dose (TID) of the order of 300 Mrad. Hence, further optimisation of the pixel circuitry and the readout architecture will be needed to achieve the required integrated radiation tolerances as well as to shrink the pixel pitch to 10 μm. Moreover, the on-chip circuitry will need to be optimised to handle the data rate of the VD. Finally, concerning the hit time resolution, the target value has already been approached on ITS3 prototypes [9].

For the ML and OT, the pixel pitch will be increased to about 50 μm to limit the power budget below 30-50 mW/cm^2 and keep the services (power supply and cooling) well constrained in terms of material budget ($< 1\%\ X_0$ per layer). However, further studies are needed to verify whether a larger pixel pitch offers significant advantages in the 65-nm technology node with a thin epitaxial layer of about 10 μm. Another common area of R&D for ML and OT, related to

the very large detector surface, focuses on the implementation of an industrialization process of the module production as well as module testing automation.

For both VD and ML, R&D has to be carried out to facilitate the system integration and reduce the amount of ancillary components within the detector acceptance. For example, on-chip serial powering will be an important asset to keep the material budget withing specifications.

The baseline technology for the data transmission is the Versatile Link PLUS [10] which will allow the transition from electrical to optical signal transmission inside the detector volume. For the VD, the radiation load as well as operation in vacuum likely necessitates to move the electrical-to-optical transition further away from the detector or to use an alternative technology like the silicon photonics being studied in the context of CERN EP R&D [11, 12].

2.2 Silicon-based time-of-flight detector

The time-of-flight system consists of an inner TOF barrel (iTOF) located at $r = 19$ cm, an outer TOF barrel (oTOF), located outside the last tracker layer, at $r = 85$ cm, and forwards disks (fTOF), after the last tracker disks, at $|z| = 370$ cm, covering a total area of 44.5 m^2 and a pseudorapidity acceptance $|\eta| < 4$.

2.2.1 Specifications

The main sensor specifications are given in Tab. 2. The quoted time resolution is for the full detector system, i.e. the sensor requirement is more stringent and an adequate (i.e. below 10 ps jitter) timing distribution system is required.

Table 2: TOF specifications.

	Inner TOF	Outer TOF	Forward TOF disks
Area (m^2)	1.5	37	6
Granularity (mm^2)	1×1	5×5	1×1 to 5×5
Hit rate (kHz/cm^2)	200	15	280
Material budget (%X_0)	1 to 3	1 to 3	1 to 3
Power density (mW/cm^2)	50	50	50
System time resolution (ps)	20	20	20
Radiation tolerance NIEL (1 MeV n_{eq}/cm^2)	$7 \cdot 10^{12}$	$9 \cdot 10^{11}$	$1 \cdot 10^{13}$
Radiation tolerance TID (rad)	$3 \cdot 10^5$	$2 \cdot 10^4$	$4 \cdot 10^5$

2.2.2 Baseline sensors and additional options

The R&D for the TOF focuses on three sensor technologies: fully depleted CMOS sensors, Low Gain Avalanche Detectors (LGADs) and Silicon Photomultipliers (SiPMs).

Fully depleted CMOS sensors are taken as the baseline R&D target, since a monolithic sensor design is expected to significantly reduce the fabrication costs compared to traditional hybrid designs, offering at the same time a simpler and cheaper assembly. To achieve the requirements, the time resolution of CMOS sensors needs to be pushed significantly beyond the present state-of-the-art by implementing a thin gain layer, for which a targeted R&D is required.

In the recent years, high resolution timing systems based on LGADs have reached full maturity, and state-of-the-art devices with a thickness of 25 μm, 35 μm and 50 μm offer a time resolution that can reach 22 ps at sensor level [13]. LGADs are produced on sensor-grade silicon wafers and

require dedicated readout electronics. This leads to higher production cost and more complex assembly procedures as compared to monolithic sensors. For these reasons, hybrid LGADs are considered as a fall-back solution.

An alternative approach using SiPMs has been investigated in a series of beam tests of different sensors [14–16]. For charged particles traversing the sensors, Cherenkov radiation that is generated in the protection layer induces large signals, leading to an efficiency near 100% and a time resolution around 20–25 ps. However, simulations of expected radiation load at the positions where the two TOF layers and two disks will be located, makes this option impractical for the inner TOF and the two disks. As a consequence, this solution will be further pursued only for the outer TOF layer. The use of SiPMs for TOF measurements may open the possibility to combine the functionality of the outer TOF RICH in a single detector system, as discussed in Section 2.3.

2.2.3 R&D plans

The TOF R&D is focused on approaches that are fully compatible with baseline CMOS technologies in order to minimise cost. A first attempt to add a gain layer to an otherwise standard quadruple well CMOS Imaging Sensor (CIS) process has been carried out thanks to a collaboration between ALICE and the ARCADIA project, an INFN-funded R&D initiative targeting the development of advanced CMOS sensors for particle detection applications. Results obtained from the characterization of prototype sensors from a first engineering run are very promising as a time resolution of 75 ps has been measured in sensors of 50 μm thickness [17], to be compared with the target value of $\sim$ 20 μm for optimized timing performance in the final sensor. A three–years R&D program focused on sensor thickness and layout optimization, and on-chip FEE design is planned to advance this technology to a level suitable for equipping the TOF layers.

2.3 SiPM-based RICH detector

The RICH detector consists of aerogel radiator tiles coupled to SiPM photodetectors by a proximity gap of about 20 cm, arranged in a barrel (bRICH), at an inner radius $r = 90$ cm, and forward disks (fRICH), at a longitudinal position $|z| = 380$ cm, covering a total area of 37 m^2. Surrounding the outer TOF barrel, the bRICH covers a pseudorapidity range of $|\eta| < 2.0$, spanning a total length of 7 m, with a radial extent from 0.9 to 1.2 m. The two end-caps of the fRICH cover the pseudorapidity regions $-4 < \eta < -2$ and $2 < \eta < 4$, respectively. The Cherenkov radiator comprises hydrophobic aerogel tiles ($15 \times 15 \times 2$ cm^3, refractive index $n = 1.03$). The photo-detection layer, positioned 20 cm from the radiator, relies purely on proximity focusing to image the Cherenkov ring. This setup allows extending the electron/pion separation from 500 MeV/c (TOF limit) to about 2 GeV/c and charged hadron identification (3 σ proton/kaon separation) up to about 10 GeV/c.

2.3.1 Specifications

The main sensor specifications are given in Tab. 3.

2.3.2 Baseline sensors and options

The proposed photon detector consists of a SiPMs layer connected to the Front-End Electronics (FEE) layer via a ceramic interposer integrating microchannels for evaporative CO_2 cool-

Table 3: RICH SiPM sensor specifications.

	Barrel RICH	Forward RICH disks
Area (m^2)	28	9
Granularity (mm^2)	2×2	2×2
Hit rate (kHz/cm^2)	15	280
Photon detection efficiency at 400 nm (%)	40	40
Material budget ($\%X_0$)	1 to 3	1 to 3
Power density (mW/cm^2)	50	50
Time resolution (ps)	50	50
Radiation tolerance NIEL (1 MeV n_{eq}/cm^2)	$6.2 \cdot 10^{11}$	$1 \cdot 10^{13}$
Radiation tolerance TID (rad)	$1.5 \cdot 10^4$	$3 \cdot 10^5$

ing.

Option with time-of-flight measurement implemented in RICH
R&D studies are ongoing to explore the possibility to use SiPMs to measure the arrival time of charged particles thus allowing the use of the same sensor layer for both Cherenkov photon detection and TOF measurements, significantly reducing the total cost of the apparatus. The concept of the Cherenkov-based TOF system could be achieved by having, in front of the SiPMs, a thin layer (1-2 mm) of solid Cherenkov radiator (e.g. SiO_2, MgF_2, or high-refractive-index glass) and exploiting the time information of the Cherenkov photons to measure the TOF of the charged particle. The time resolution is proportional to $\sqrt{1/N}$, where N is the number of fired SiPM cells, and could reach the required target of 20 ps for the expected values of $N > 5$ [18].

Option using HRPPD as photon detector in the fRICH
The expected radiation exposure in the fRICH region is approximately $3.9{\cdot}10^{13}$ 1 MeV n_{eq}/cm^2. SiPM operation surpassing 10^{13} 1 MeV n_{eq}/cm^2 results in a notable increase in Dark Count Rate (DCR) to levels exceeding tens of MHz/mm^2, which will prevent single photon detection. However, this radiation load has a much reduced impact on the operation of vacuum-based devices, in particular the High-Resolution Picosecond Photo Detectors (HRPPD) [19–21], which feature exceptional time resolution and low DCR, rendering them ideal candidates for photon detection in the fRICH.

2.3.3 R&D plans

The R&D will mainly focus on the SiPMs, the associated read-out electronics and the photodetector module.

The performance of the RICH system is strongly driven by the SiPM parameters, particularly the photon detection efficiency (PDE) and the DCR, which directly affect single photon statistics and time jitter. Therefore, it is of paramount importance to limit the increase of the DCR due to radiation damage to below 1 MHz/mm^2 by operating the RICH system at $-40\,^{\circ}C$, combined with annealing cycles at temperatures around +50 °C during the LHC winter shutdowns. This approach requires detailed engineering studies to account for mechanical stress, tolerances, long-term reliability, etc. As complementary approach, an R&D project is being launched in collaboration with Fondazione Bruno Kessler (FBK) for the development of SiPM optical en-

trance textures made by micro-lens arrays (MLAs) in order to focus the Cherenkov photons onto the centre of each SPAD. This, together with the choice of small SPAD sizes reduces the surface exposed to radiation damage. The implementation of MLAs results in an increase of the PDE by 22% and a reduction of the cross-talk by 40 % [22]. The focusing results also in an improvement of the single photon time resolution, as observed in [23] where 28 ps FWHM have been measured in optimized SiPMs NUV-HD-CHK by FBK with metal masks integrated in the micro-cell borders to remove the contributions from slower regions inside the sensor structure.

Moreover, progress in 3D interconnecting technologies based on TSV (through-silicon vias) is leading to a new generation of SiPMs: hybrid devices combining the integrated functionalities of the digital SiPM with the high performance of custom technologies, like low noise and high detection efficiency [24].

3 R&D on mechanics and cooling for a retractable vertex detector and on robotic installation tooling

Dedicated R&D is needed for the development of the vertex detector mechanics, which is pushing the limits of several existing technologies, including vacuum systems, 3D printing, cooling, and the manufacturing of ultrathin walls. Additionally, a modular design for all sub-detectors is being considered, with the goal of enabling fast installation and precise positioning via a robotic system.

3.1 Mechanics and cooling of the retractable vertex detector

To be as close as possible to the interaction point, the tracker is placed into a secondary vacuum inside the beampipe and is mounted such that it can be retracted during LHC injection for a minimum required aperture of 16 mm and moved close to the interaction point for data taking with stable beams at 5 mm. Compared to the existing LHCb VELO [25], a tracker covering a large acceptance including the mid-rapidity region requires a design that minimises the amount of material in all directions. This is new terrain and will require dedicated R&D activities in order to achieve the required mechanical stability. The system is further constrained by impedance and vacuum stability requirements at the interaction points inside the LHC experiments.

An on-detector active cooling is required to cool the sensors (power dissipation $\sim$70 mW cm^{-2}) and the heat generated by the LHC beam with the secondary vacuum walls ($\sim$90 mW cm^{-2}). Two-phase evaporative CO_2 cooling is currently assumed to be the baseline cooling technique. While this is an established solution, in use or foreseen for the other trackers at the LHC [25–28], R&D has been launched to study ultra-light mini/micro channel cooled coldplate to efficiently remove heat and to assure the proper operation temperature for the sensors, despite increased leakage currents induced by radiation. Preliminary thermal simulations indicate that such a design allows the operation of the vertex detector at -25 °C with a temperature spread across the silicon surface below 5 °C.

3.2 Robotic systems for detector maintenance and installation

Activities are already in progress to develop robotic systems for the automated handling, maintenance, and installation of detector modules which will ensure precise and controlled installation and will significantly reduce maintenance durations.

R&D efforts have also been directed towards the development of a motion controller for the retraction during the beam injection of the vertex detector placed at a few millimeters from the interaction point. The opening and closing of the tracking system is expected to be performed by a rotatory magnetic feedthrough, a device that uses a high flux magnetic coupling to move a rotor inside the beam pipe while preserving the vacuum integrity. Reliability is currently under investigation, and a control system featuring motor encoder and limit switches has been developed to ensure safe operation.

Moreover, given the retractable vertex detector's high exposure to intense radiation, more frequent maintenance is expected. Preliminary design concepts for the automatic extraction and insertion of this tracking system have been proposed, aiming at preserving the integrity of the beam pipe vacuum while avoiding the disassembly of other detector modules.

The development of these new areas will require further R&D efforts and focused activities to assess the feasibility and performance of the robotic jig design, to validate the reliability of the retractable vertex tracker's opening and closing mechanism, and to enhance and test its automatic extraction process.

4 R&D plans for the other ALICE 3 subsystems: MID, FD, ECal

The MID is located outside the magnet, covers $|\eta| < 1.3$, and consists of a hadron absorber followed by sensor planes made of plastic scintillator bars coupled to SiPMs, or alternatively by resistive plate chambers (RPC) or multiwire proportional chambers. The minimum required granularity is $\approx 5 \times 5\,\mathrm{cm}^2$. Although the different technologies that are proposed for MID are well established, R&D is required to make sure that the following specific requirements are met: time resolution better than 100 ns; radiation tolerance to NIEL of 1.7×10^{10} $1\,\mathrm{MeV\,n_{eq}/cm^2}$; efficiency close to 100%; an eco-friendly gas, in the case of the RPC option. Technology surveys and test-beam campaigns with small-scale prototypes are already ongoing.

The FD at $4 < |\eta| < 7$ will consist of two segmented discs made of plastic scintillators, with light collection through clear fibres attached to photomultipliers (PMTs). The readout of the FD requires FEE for recording collision events every 25 ns. The radiation tolerance should be up to 50 Mrad and 5×10^{14} $1\,\mathrm{MeV\,n_{eq}/cm^2}$. For the plastic scintillators the Eljen technology is currently considered, possibly with increased dopant concentration to further improve radiation tolerance. Another option is the usage of intrinsically radiation-hard Polyethylene Terephthalate or Polyethylene Naphthalate scintillators [29]. Fine-mesh PMTs from Hamamatsu are the primary choice for the photon sensors. Another option is the usage of microchannel plate (MCP) PMTs with atomic layer deposition of aluminium and magnesium oxide (Al_2O_3+MgO) [30]. R&D will focus on the FEE development and prototype tests for scintillators and PMTs.

The barrel ECal calorimeter is installed inside the solenoid magnet at $|\eta| < 1.6$. A one-side endcap covers $1.6 < \eta < 4$. The barrel comprises a high-precision segment built with re-used lead tungstate crystals ($PbWO_4$) of the present ALICE PHOS, and larger segments made of standard sampling Pb-scintillator cells. The choice of adequate photodetectors based on SiPM is driven by the expected optical photon flux on the unit surface and the dynamic range of the signals. There are multiple vendors of SiPM with suitable parameters. Dedicated R&D is needed

Table 4: Comparison of silicon pixel sensor specifications for the ALICE ITS3, ALICE 3 Vertex Detector and Tracker, ePIC at EPIC [31], and FCC-ee detector.

	ITS3	ALICE 3 VTX	ALICE 3 TRK	ePIC	FCC-ee
Single-point res. (μm)	5	2.5	10	5	3
Time res. (ns RMS)	2000	100	100	2000	20
In-pixel hit rate (Hz)	54	96	42		few 100
Fake-hit rate (/pixel/event)	10^{-7}	10^{-7}	10^{-7}		
Power cons. (mW / cm^2)	35	70	20	$<$40	50
Hit density (MHz/cm^2)	8.5	96	0.6		200
NIEL (1 MeV n$_{eq}$/cm^2)	$4 \cdot 10^{12}$	$1 \cdot 10^{16}$	$2 \cdot 10^{14}$	few 10^{12}	10^{14} (/year)
TID (Mrad)	0.3	300	5	few 0.1	10 (/year)
Material budget (X_0/layer)	0.09%	0.1%	1%	0.05%	˜0.3%
Pixel size (μm)	20	10	50	20	15-20

to establish the technology to reshape $PbWO_4$ crystals with the required taper for ALICE 3. To ensure high light yield and high energy resolution, the $PbWO_4$ cells need to be cooled to -25°C with temperature stabilisation $\sigma_t = 0.1^\circ$C, as achieved for the PHOS operation in ALICE.

5 Connections and synergies with ECFA silicon detector R&D

The R&D directions for the silicon-based ALICE 3 sensors have a large overlap with those for the EIC experiments, which are on the same timescale as ALICE 3, as well as experiments at lepton collider options (ILC, FCC-ee, CLIC, Muon Collider) in the more distant future. This overlap is illustrated in Fig. 2 from the 2021 ECFA Detector R&D Roadmap [3]. The strongest priorities for ALICE 3 (red symbols) are position precision, low material budget (x/X_0), low power and large-area sensors for trackers, as well as ultra-fast timing for time-of-flight measurement and radiation tolerance for the SiPM sensors. These match the priorities for future lepton colliders. The quantitative target specifications for pixel sensors, reported in Tab. 4, are similar for what concerns position resolution (2.5 and 10 μm for the VD and OT, respectively), material budget (0.1 and 1% of X_0, respectively), and power consumption (70 and 20 mW/cm^2, respectively) as well as hit densities of the order of 100 MHz/cm^2.

The key R&D goals for ALICE 3 align significantly with goals and activities of the ECFA Detector R&D groups DRD3/DRD7 (for the Inner Tracker and Outer Tracker sensors), and DRD4 (for the RICH sensors and radiation damage mitigation). The ALICE collaboration fully supports collaborative R&D in this context.

In summary, the R&D program for ALICE 3 will advance sensor technology in directions that have clear synergies with other programs in the near (e.g. EIC) and more distant (FCC-ee) future. The ongoing development program can serve as a concrete mid-term milestone in the longer-term roadmap. The R&D for ALICE 3 outlined in this document is therefore an integral part of the strategic roadmap for detector development.

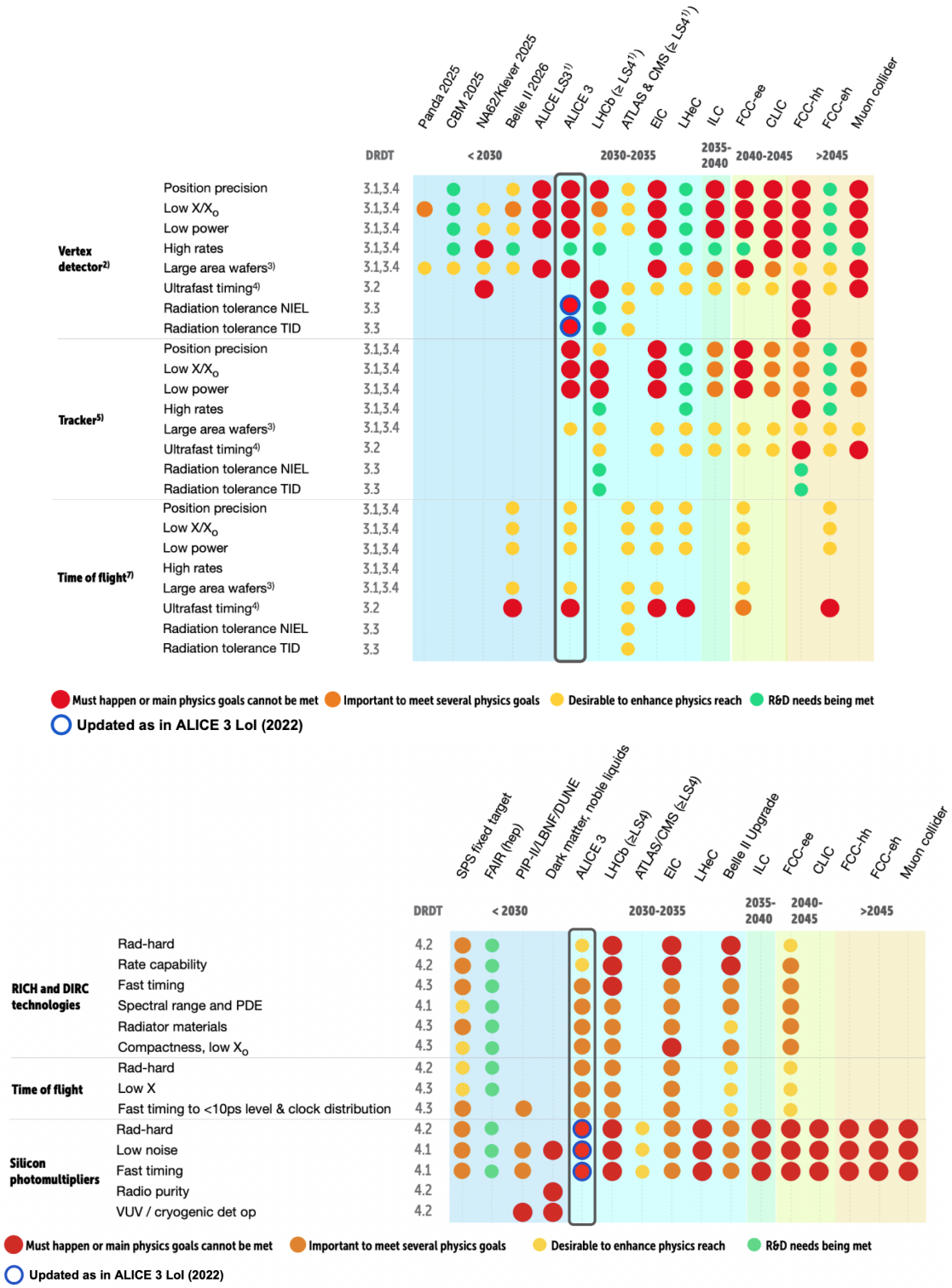

Figure 2: Summary of R&D goals and priorities for future silicon sensors (upper table) and PID detectors (lower table). The tables are adapted from 2021 ECFA detector R&D roadmap [3] with some updates based on the ALICE 3 Letter of Intent [1].

References

[1] **ALICE** Collaboration, "Letter of intent for ALICE 3: A next-generation heavy-ion experiment at the LHC, CERN-LHCC-2022-009, LHCC-I-038", arXiv:2211.02491 [physics.ins-det].

[2] **ALICE** Collaboration, "Scoping document for the ALICE 3 detector, CERN-LHCC-2025-002, LHCC-G-185", tech. rep., CERN, Geneva, 2025. https://cds.cern.ch/record/2925455.

[3] ECFA Detector R&D Roadmap Process Group, "The 2021 ECFA detector research and development roadmap, CERN-ESU-017", tech. rep., Geneva, 2020. https://cds.cern.ch/record/2784893.

[4] **ALICE** Collaboration, "Technical Design Report of the ALICE Inner Tracking System 3 - ITS3: a bent wafer-scale monolithic pixel detector, CERN-LHCC-2024-003, ALICE-TDR-021", tech. rep., 2024. https://cds.cern.ch/record/2890181.

[5] B.-H. Lim on behalf of the ALICE collaboration, "Thin monolithic pixel sensors with fast operational amplifier output in a 65 nm imaging technology for ALICE ITS3", *Nucl. Instrum. Meth. A* **1055** (2023) 168478. https://www.sciencedirect.com/science/article/pii/S0168900223004680.

[6] G. A. Rinella *et al.*, "Time performance of analog pixel test structures with in-chip operational amplifier implemented in 65 nm cmos imaging process", *Nucl. Instrum. Meth. A* **1070** (Jan., 2025) 170034. http://dx.doi.org/10.1016/j.nima.2024.170034.

[7] G. Borghello *et al.*, "Optimization of monolithic pixel sensors for high energy physics applications using 3D TCAD simulations", *Proceedings of PIXEL2024, in preparation* (2024) .

[8] G. A. Rinella *et al.*, "Digital pixel test structures implemented in a 65 nm CMOS process", *Nucl. Instrum. Meth. A* **1056** (2022) 168589, arXiv:2212.08621 [physics.ins-det].

[9] G. Aglieri Rinella *et al.*, "Digital pixel test structures implemented in a 65 nm cmos process", *Nucl. Instrum. Meth. A* **1056** (2023) 168589. https://www.sciencedirect.com/science/article/pii/S016890022300579X.

[10] C. Soós *et al.*, "Versatile link plus transceiver development", *Journal of Instrumentation* **12** no. 03, (Mar, 2017) C03068. https://dx.doi.org/10.1088/1748-0221/12/03/C03068.

[11] C. Joram et al., "Extension of the R&D Programme on Technologies for Future Experiments", tech. rep., CERN, 2023. https://cds.cern.ch/record/2850809.

[12] J. Troska, F. Vasey, and A. Weidberg, "Radiation tolerant optoelectronics for high energy physics", *Nucl. Instrum. Meth. A* **1052** (2023) 168208. https://www.sciencedirect.com/science/article/pii/S0168900223001985.

[13] F. Carnesecchi *et al.*, "A new Low Gain Avalanche Diode concept: the double-LGAD", arXiv:2307.14320 [physics.ins-det].

[14] F. Carnesecchi *et al.*, "Direct detection of charged particles with SiPMs", *Journal of Instrumentation.* **17** no. P06007, (2022) .

[15] F. Carnesecchi *et al.*, "Understanding the direct detection of charged particles with SiPMs", *Eur. Phys. J. Plus* **138** (2023) 337.

[16] F. Carnesecchi *et al.*, "Measurements of the Cherenkov effect in direct detection of charged particles with SiPMs", *Eur. Phys. J. Plus* **138** (2023) 788.

[17] U. Follo *et al.*, "First results on monolithic cmos detector with internal gain", *Journal of Instrumentation* **19** no. 07, (Jul, 2024) P07033. https://dx.doi.org/10.1088/1748-0221/19/07/P07033.

[18] N. Nicassio *et al.*, "A combined SiPM-based TOF+RICH detector for future high-energy physics experiments", in *2023 9th International Workshop on Advances in Sensors and Interfaces (IWASI)*, pp. 199–204. 2023.

[19] B. W. Adams and et al., "A Brief Technical History of the Large-Area Picosecond Photodetector (LAPPD) Collaboration", (3, 2016) . https://www.osti.gov/biblio/1294432.

[20] M. Barnyakov *et al.*, "Latest feasibility studies of LAPPD as a timing layer for the LHCb Upgrade 2 ECAL", *Journal of Instrumentation* **19** no. 02, (Feb, 2024) C02045. https://dx.doi.org/10.1088/1748-0221/19/02/C02045.

[21] J. Agarwala, "Timing resolution of a LAPPD prototype measured with CERN PS test beams", *Nucl. Instrum. Meth. A* **1069** (2024) 169838. https://www.sciencedirect.com/science/article/pii/S0168900224007642.

[22] G. Haefeli *et al.*, "Microlens-enhanced SiPMs", arXiv:2411.09358 [physics.ins-det].

[23] S. Gundacker *et al.*, "On timing-optimized SiPMs for Cherenkov detection to boost low cost time-of-flight PET", *Physics in Medicine Biology* **68** no. 16, (Aug, 2023) 165016. https://dx.doi.org/10.1088/1361-6560/ace8ee.

[24] L. Parellada-Monreal *et al.*, "3d integration technologies for custom sipm: From bsi to tsv interconnections", *Nucl. Instrum. Meth. A* **1049** (2023) 168042. https://www.sciencedirect.com/science/article/pii/S0168900223000323.

[25] **LHCb** Collaboration, *LHCb VELO (VErtex LOcator): Technical Design Report*. Technical design report. LHCb. CERN, Geneva, 2001. https://cds.cern.ch/record/504321.

[26] **ATLAS** Collaboration, "Technical Design Report for the ATLAS Inner Tracker Pixel Detector, CERN-LHCC-2017-021, ATLAS-TDR-030", tech. rep., CERN, Geneva, 2017. https://cds.cern.ch/record/2285585.

[27] **CMS** Collaboration, "CMS Technical Design Report for the Pixel Detector Upgrade, CERN-LHCC-2012-016, CMS-TDR-11", tech. rep., 2012. https://cds.cern.ch/record/1481838.

[28] **LHCb** Collaboration, "LHCb VELO Upgrade Technical Design Report, CERN-LHCC-2013-021, LHCB-TDR-013", tech. rep., 2013. https://cds.cern.ch/record/1624070.

[29] P. Conde Muíño *et al.*, "Production and optical characterisation of blended polyethylene terephthalate (pet)/polyethylene naphthalate (pen) scintillator samples", *Nucl. Instrum.*

Meth. A **1066** (Sept., 2024) 169627.
http://dx.doi.org/10.1016/j.nima.2024.169627.

[30] D. Miehling *et al.*, "Lifetime and performance of the very latest microchannel-plate photomultipliers", *Nucl. Instrum. Meth. A* **1049** (2023) 168047.
https://www.sciencedirect.com/science/article/pii/S0168900223000372.

[31] **ePIC Silicon Vertex Tracker Detector Subsystem** Collaboration, L. Gonella, "Development of a Silicon Vertex and Tracking Detector for the Electron-Ion Collider", *PoS* **VERTEX2023** (2024) 038.